
Proceedings Paper:
Olugbenga, AG, Antony, SJ, Nasir, A et al. (2022) Experimental DEM Hybrid Approach for Prediction of Landslide in Ughelli Sandstone. In: Lecture Notes in Electrical Engineering. World Congress on Engineering 2021, 07-09 Jul 2021, London, U.K. Springer Singapore, pp. 87-100. ISBN: 9789811935787. ISSN: 1876-1100. EISSN: 1876-1119.

https://doi.org/10.1007/978-981-19-3579-4_7

Experimental-DEM Hybrid Approach for Characterizing Micromechanical Strength of Ughelli Sandstone

A. G. Olugbenga, S. J. Antony, A Nasir, M. U. Garba and M. D. Yahya

***Abstract*—Landslide has occurred in Nigeria recently, this has necessitated the simulation of crack number associated with tensile failures in sandstone subjected to tri-axial compressions. The aim is to relate the crack number to microscopic deformation which is the extent of isotropic and deviatoric components of the simulated seismic crack number to the microscopic failure mechanisms. Within the rock matrix, the cataclastic collapse occurs as the granular arrangement interferes with the applied forces which initiate a strong spatial anisotropic stress field depending on the level of applied force. The onset of the micro-cracking initiates the occurrence of the rock failure. The crack number was recorded simultaneously as the grain-to grain contacts breaks the montmorillonite mineral bond between the quartz grains. Experimental data were plotted as the contact strength reduces by tri-axial stresses induced on the rock, so that within the invisible cracks, a significant fraction of isotropic percentage in all directions were captured. The stress induced on the sample by axial and radial compression affect the waveforms and the recorded crack number are simultaneous. This micro-crack numbering provided microscopic deterioration between 5MPa to 25MPa, at this stress level no visible fracture occurring in the macroscopic feature was seen. This was achieved by representing the physical sandstone grain with an assembly of clump particle during procedural simulation of the sandstone. Thus, the interactions between clumps were governed by the defined micro-properties of spheres making the clumps. The strain in the sandstone was represented by a stiffness ratio of 1 which is in agreement with experimentally determined stiffness ratio obtained from the natural sandstone.**

***Keywords*— sandstone, simulation, tri-axial stress, crack-number, macro-fracture.**

Manuscript received March 05, 2020; revised March 13, 2020. This work was supported by TETFUND and PTDF (I acknowledged Nigeria's sponsor and financial support). Adeola Grace Olugbenga, Simon Joseph. Antony, Abdulkarim Nasir, Mohammed Umar Garba and Muibat Diekola Yahya

A. G. Olugbenga is with the Department of Chemical Engineering, School of Infrastructure, Process and Engineering Technology, Federal University of Technology Minna. Department of Chemical Engineering (Phone: +2349063533503; fax: +234 (66) 224482; e-mail: grace.adeola@futminna.edu.ng).

S. J. Antony is with University of Leeds, School of Chemical and Process Engineering, Leeds, Engineering Building, University of Leeds, 211 Clarendon Rd, Woodhouse, Leeds LS2 9JT, United Kingdom (e-mail: S. J. Antony@leeds.ac.uk).

A. Nasir is with the Mechanical Engineering Department, School of Infrastructure, Process and Engineering Technology, Federal University of Technology, Minna, (e-mail: a.nasir@futminna.edu.ng). M. U. Garba is with the Department of Chemical Engineering, School of Infrastructure, Process and Engineering Technology, Federal University of Technology Minna, Department of Chemical Engineering, (e-mail: umar.garba@futminna.edu.ng). M. D. Yahya is with the Department of Chemical Engineering, School of Infrastructure, Process and Engineering Technology, Federal University of Technology Minna, Department of Chemical Engineering, (e-mail: muibat.yahya@futminna.edu.ng).

I. Introduction

THE elastic waves produced spontaneously due to the micro-fracturing of rock under stress are referred to Acoustic emissions (AE). The AE waveforms are directly represented as crack number in discrete element modelling (DEM) and thus, counting them can be used to describe the mechanism of silent micro fracture processes. Eberhardt et al (1998) has presented the use of acoustic emissions to provide deformation in granite. The deformation mechanisms in other brittle materials can be understudied by the research done by Graham et. Al., (2010). Thus the study of damage thresholds and crack accumulation in rock is evolving in order to reveals the behaviour of brittle materials under natural and physical conditions. Martins (1994) stated that, by taking the stress-strain behaviour of uniaxial compressive stress (UCS) tests into log space (stress vs. log strain) will highlight different damage thresholds. While all the damage thresholds crack initiation (CI), crack damage (CD) and peak strength are coincidental for a single test but using the direct tensile method, they can be more readily distinguished in a Brazilian test. Furthermore Matins (1994) represents the first notable deviation from linearity in a log space curve of stress strain as the initiation of the first crack in the specimen; the next was taken as the onset of systematic damage that is coincident with volumetric strain reversal. Thus the next point of deformation was interpreted as the crack coalescence and yielding limit which preceded rupture or splitting. Some other examples are the mechanisms understudied in brittle materials such as rocks and concretes have employed the use of AE for process definition one of such description is the procedure provided by Lockner et al., (1991), the procedure they adopted included slowing down macroscopic failure of granite whereby acoustic emissions were used as feedback control to the stress applied. Some applications of fracture mechanism included deformation occurring by pore pressure caused by injection of fluid Stanchits et al., 2011, (Heinze, et al., 2015)., compaction band has been used to defined the mechanism of deformation Fortin et al., 2006, Cho et al (2008)], the evolving breakouts in boreholes Dresen et al., 2010, macroscopic fractures under polyaxial loads Young, et al., 2012. There is a direct application to the understanding of fracture mechanism which is to predict the mechanical behaviour of granular structures (such as rocks) in stressed environments. However, fundamental limitations for fracture modelling still exist and must be addressed.

The limitations to fracture predictions in Nigeria's sandstone are compounded because the fractures occur in-situ and no existing data are available for wide area examinations, this may accounts for land slides which are probably a gradual process of granular distortion. The starting point is crack initiation to final collapse. Landslides has been reported last year in the dailies in Nigeria, because of the several drilling of water borehole within the built metropolis, hence the motivation is to obtain an immediate possible description of failure mechanism. So as to suggest necessary precautions to drillers.

Regardless of geometry in the Ughelli water boreholes, mechanical stress in the vicinity of the hole display complex deformation mechanisms because of the complex stress field. Core samples of natural rock were obtained from water boreholes. By using the same dimensions of the natural core sample, a mathematical sample was simulated. A top pattern was run for the load applications which induced strain into the rock. This causes the clumped assembly of particles to form a spatial and dependent anisotropic strain distribution in the rock matrix initiating the micro-cracks exhibited as tensile before the shear failures. Every crack between particle-to-particle contacts was numbered for spatio-temporary evolution of acoustic until visible crack was noticed. The cracking event were related to macroscopic axial-stress. The plots of confined stress were obtained as sigma 1, sigma 2 and sigma 3 to study the behaviour of the sandstone. Full profile of micro-cracks were segmented to indicate damage mechanisms similar to the seismic moment tensors which proved to be a useful tool for quantitative strength characterization of rocks.

To insert images in *Word,* position the cursor at the insertion point and either use Insert | Picture | From File or copy the image to the Windows clipboard and then Edit | Paste Special | Picture (with "float over text" unchecked).

II. EXPERIMENT AND MODELLING FOR MICROMECHANICAL CHARACTERIZATION OF UGHELLI SANDSTONE

A. Sample Preparation

A 38mm diameter and 90mm by height of sandstone core samples were taken from Ughelli in Nigeria. Foremost, an experiment was carried out to determine the stiffness ratio of micro-parameters of normal to shear stiffness (kn/ks) at the contact between grain to grain in the sandtone sample (figure 1). details of this procedure is found in Antony, et al.,(2017). The stiffness ratio was consistent with the corresponding Poison's ratio of the 52 samples tested. By using the stiffness ratio, a mathematical sample was synthesised by generating randomly shaped clump with a range of sizes to create a bonded particle model. The sample was dimensioned 30mm by 90mm (the vessel is equivalent to the laboratory cell) for the purpose of simulating unconfined compressive strength (UCS) and confined tests on bonded granular structure. A compressive test which was simulated in a cylindrical sleeved tri-axial vessel. the top and bottom walls work as loading platens and the side walls provide the confinement. The side walls keep the confining pressure constant, by changing the velocity or radius in cylindrical vessels and by using a servomechanism. For the UCS test, all the sidewalls will be removed. The following steps will be taken for conducting a compression test (Itasca 2004).

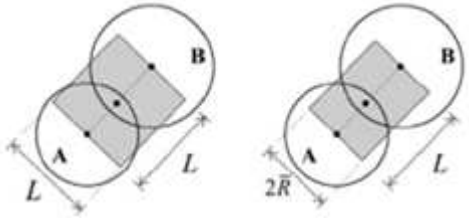

Fig. 1. Grain and parallel bond elastic

(Potyondy and Cundall 2004). Each particle was made small enough to represent natural sandstone so that the crack propagates through its natural path. This does not allow the creation of a tortous path. The crack number were recored in order to obtain the corresponding stress and strain data measurement sphere were used.

Measurement stress and strain for mathematical sample

The stress and strain in the samples were measured using the measurement spheres. The strain rate also was measured by the means of measurement spheres, this parameter were used for calculating Poisson's ratio in the UCS test which tally with stiffness ratio. Fig. 2.

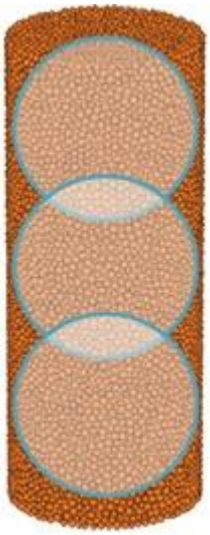

Fig. 2. Position of measurement sphere in the sandstone sample

B. Model calibration Performed on Sample

When the macro-scale properties (Poisson's ratio and Modulus) became equivalent to those those measured in the laboratory and were implemented in the codes by assigning different material properties to different parts of a model. The mathematical model directly characterize the desired behaviour of the natural rock, the model was calibrated and the stiffness ratio, the normal parallel bond, the shear bond were recorded. The calibration of mathematical model

yielded radius ratio of particle size targeted at achieving the strength properties (UCS) of the natural rock

III. DISCUSSION OF RESULTS

While the standard UCS test ends as shear fracture, the crack numbering takes into account all grain contact that gradually gests disassociated before the micro-fracturing occurs. Thus the total number of dissociated grain contact is recorded within the rock as tensile and shear compressive motion of each particle that make up the rock materials. This phenomenon yielded the crack number that are plotted in figure 3 and 4.which clearly indicated the deformation mechanisms of brittle rock under uniaxial (figure 5 and tri axial compression of rock figure 6.

Nasvis et al (2012) has used the AET, for finding damage thresholds, here the crack number were computed for. This was done so that as crack number will be recorded and compared to counts in AE events the numbering were directly associated with the expected failure mechanisms. The estimated stiffness ratio of the micro-parameters of normal to shear stiffness (kn/ks) is 1 from all experiments. This value was in agreement with the stiffness ratio obtained for the calibration of the simulated rock, this data is presented in Table 1 indicating the micro-properties of mathematical discrete model calibrated for the sandstone.

TABLE I
MICRO-MECHANICAL PROPERTIES OF UGHELLI SANDSTONE

Symbol	Micro property	Qunatity
Rmin	minimum particle radius	0.002mm
Rmin/ Rmax	particle radius ratio	1.66
pbn	Normal parallel bond	45±10 MPa
pbs	shear parallel bond	75±10 MPa
μ	Frictional coefficient	0.66
Ec	particle modulus	16GPa
Kn/ ks	stiffness ratio	1

Micro-mechanical properties obtained for Ughelli sandstone during the calibration process of the built mathematical sample.

The Rmax/Rmin is the radius ratio which yielded 1.66 after calibrating the mathematical sandstone. The corresponding normal bond strength (pbn) and shear bond strength (pbn) are 45MPa These data are the results of Ughelli sandstone samples with a height of 90m and a diameter of 30mm for the natural sandstone, for the stress-strain data obtained simulated test, observing behaviour (strain softening) near rupture a peak strength of 45MPa was recored Figure 3 and 4.

A. Macro-properties of the natural and simulated sample

The macro-properties of the natural and simulated sample is therefore fractured with visible evidence at 45MPa axial stress.

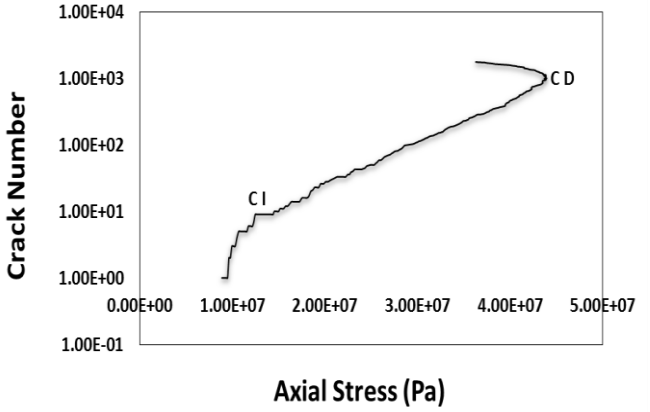

Fig. 3. Crack Initiation (CI) and crack damage (CD) stresses for unconfined axial stress application. The crack number are limited to (1x10^4) particles used for building sandstone sample in the Discrete Element Modelling (DEM).

Most of the crack number recorded prior to the failure of a sample and lack of acoustic activity in the initial stages is a concern. This explains the complicated behaviour exhibited by the rock as the initial pore collapse does not yield any crack number (Figure 5) the curves lie on the zero reading for up to a strain value of 0.0075. The strength characteristics of initial pore collapse was equally observed in the stress-strain data generated during the laboratory test carried out on the natural rock. Thus at compared to the mathematical sample, the crack number increases after the pore collapse within the clumps. A unit contact bond breakage is a unit count of the crack number. This observation describes the microstructural deformation where the onset of deformation is dictated by crack number after pore collapse. Clumps were used to represent each grain of the natural sample.

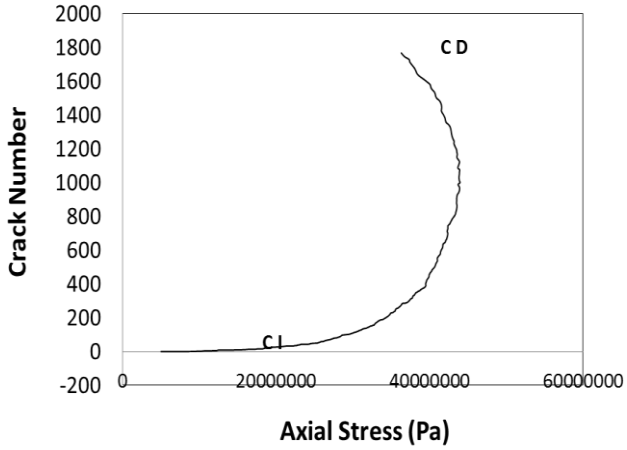

Fig. 4. Crack Initiation (CI) and crack damage (CD) stresses for unconfined axial stress application rain and parallel bond elastic.

The crack number is synonymous to the AE. Navis et al (2012) presents crack propagation thresholds obtained from acoustic emission technique. Upon the application of loading,

pre-existing micro and macro cracks in the specimen tend to close, and this phase is known as crack closure (σcc).

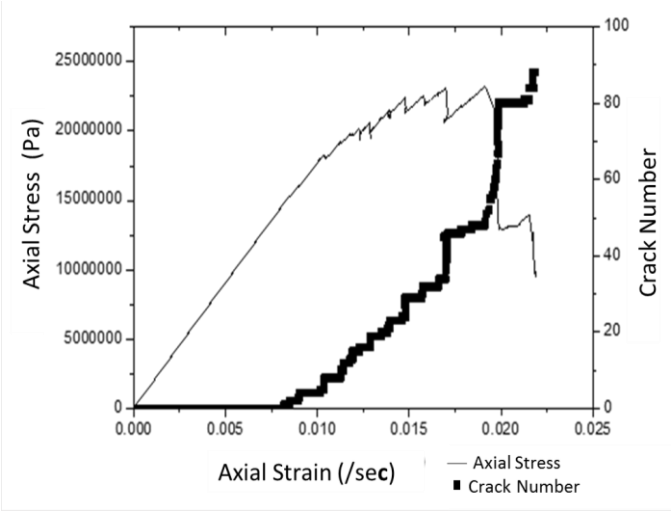

Fig. 5. Strain data and Corresponding crack number for (x10^4) particle used for simulation

During compression, very little or no acoustic activity were observed due to the crack closure of existing macro cracks because there is no release of strain energy. Crack initiation stress (σci) is defined as the point at which crack number stats to count. The count of contact breakage increase above the background level of events. This was recorded in the crack number plot made against the stress application on the mathematical rock (Figure 5) from the same plot, there was an increase in crack number in a linear manner due to the incremental loading.

In the crack number – stress curve, the crack intiation (CI) is the first point where the rate of crack number rises above zero at a starin of about 0.0075. The crack damage (CD) occurs at the point of the second sudden change in the slope. This is in agreement with the acoustic recorded curve in which the cumulative number of acoustic events was plotted against stress, Diederichs et al., (2004), also in agreement with Eberhardt et al (1998) and the reported Log "cumulative AE counts" versus Log "stress" Hazzard and Young (2000). The first point where the slope of the crack number curve rapidly changes is very obvious and can be picked with an accuracy within a short range. The crack counts that are shown in Figure 7 as crack number data are in agreement with the cumulative number of cracks number averaged from multiple cracks. This is equally in agreement with the acoustic count of the transducer readings for brittle rocks (Diederichs et al 2004, Eberhardt et al 1999).

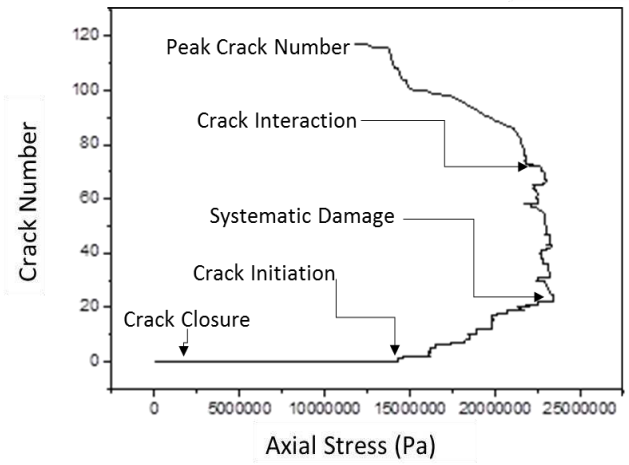

Fig. 6. Crack number and corresponding crack interaction stages: the mechanism of micro-fracturing of Ughelli sandstone at 5 stages for (x10^4) particles used for simulation

The onset of different damage levels were identified by using cumulative crack counts, which was recorded in the data output activity. The laboratory equivalent was monitored and the result is in agreement with the laboratory work reported in Figure 8, the systematic cracking as the onset of damage in the sample and crack coalescence as the starting point for localization and the yielding limit of the rock. The CD threshold can be detected by the crack number where the second change in the slope of curve occurs. The CD thresholds are presented in Figure 8, it was observed that in figures 7 and 8, the range for CD is very small. Strength characteristic of the Ughelli sandstone

The data for the unconfined compressive stress indicated only two significant points which are the crack initiation and the crack damage stresses these two were observed at 10MPa 48Mpa respectively figure 3 and 4. the systematic growth of micro-crack were not distinguished for the unconfined test therefore the confined/tri-axial test was carried out hence crack numbering were recorded and results are presented in figure 5 and 6. These figures provided clear indications of five stages of crack damage.

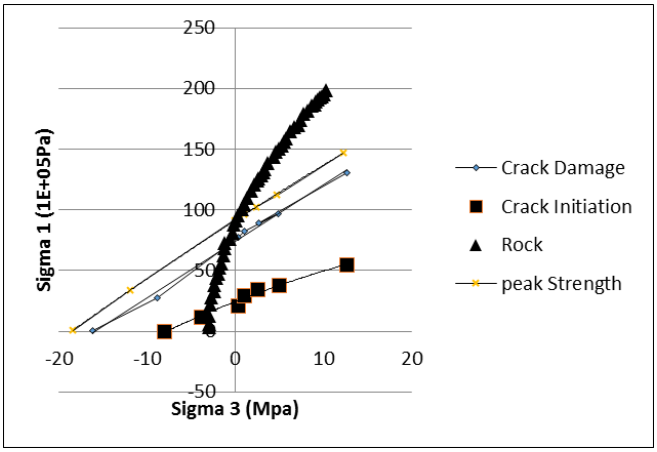

Fig. 7. Rock strength Rock Strength, Crack Initiation, Crack Damage and Peak Strength at 20MPa Confined Pressure for Ughelli sandstone under tri-axial compression

It can be seen in Figures 7 and 8 that the same sample confined at pressures of 20MPa and 25MPa respectively had an effect on the first crack and CI thresholds raising these value slightly by about 2MPa. The increases are probably caused by the internal angle of friction between grains which has been compressed/more tightly confined at 25MPa a value higher than 20MPa. Also the crack interactions, crack systematic cracks and peak strength envelopes of sandstone shift with 5MPa increase. It also can be observed that the difference in the confined pressures has no effect on the tensile strength of the sample model.

For figure 7 and 8, the negative data is a magnitude for sigma 2 that is the z-direction of stress application on the sandstone. Observe that all micro-crack data recorded are below the macro damage stress, the crack initiation stresses for x,y and z direction are at stress value below 10MPa, the systematic crack growth was observed between 10MPa and 15MPa for all axes. The crack interaction data were obtained at 18Mpa for both sigma 3 and sigma 2 (negative-x direction) and 3 (positive x-direction) while the axial y-direction was at about 70MPa. The peak stresses for the micro-cracks were observed at 18MPa for both sigma x and z while the axial y-direction was at about 90MPa. This peak of micro-crack intercept the rock strength at 90MPa where macro fracture begins. The rock sustains its strength until an axial stress on 250MPa was reached before the sample fractured. Observed that the stress in direction x and

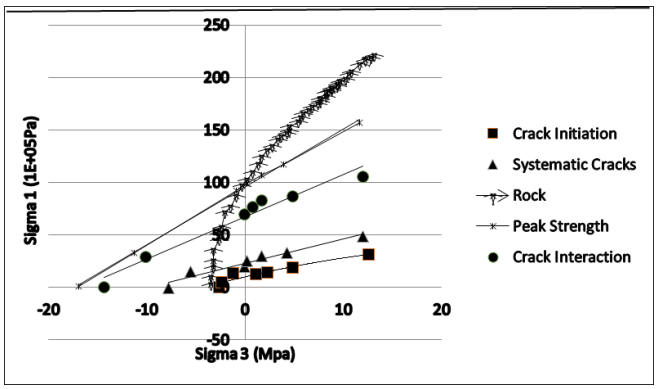

Fig. 8. Rock strength, crack initiation, crack damage and peak strength at 25MPa confined pressure for Ughelli sandstone under triaxial compression

Therefore for the Ughelli sandstone, the crack number plot in the stress strain indicated the 4 stages of micro-crack in figure 6. There was no crack numbering at less than 5MPa axial stress even though the sample was undergoing a strain up till 0.005. The first crack appear at a strain of 0.008 this is the crack initiation stage, next signature of the crack number was observed below 20MPa indication of systematic crack growth. The first peak stress was observed at about 20MPa this is the crack interaction stage. The crack continues to grow until a peak value of 225MPa was reached which coincide with the macro strength of rock under confined pressure

IV. CONCLUSIONS

Triaxial experiment carried out to investigate the source mechanisms of crack number during loading of a core sandstone sample have been presented. The dissociation of the grain to grain contact bond associated with the recorded crack shows the complexity of fracture mechanisms during failure, crack initiation, interaction, coalescence and damage because they are not visible. The observed micro-cracking rate is divided into four stages with increasing number of micro-crack, pure elastic phase were observed for standard test method. The direct implication to drillers is that Development of water borehole which breakouts and localized macroscopic shear bands occurs begins with silent micro-cracks far before the catastrophic failure. Recorded crack number follow reasonably well existing damage signatures but the elastic region of the unconfined test conceal the onset of failure in the intra-granular bonding. The peak stress from the triaxial stress coincides with the orientation of the macroscopic fractures in the sample. Crack number close to the peak stress can be probably suggested to borehole drillers not to exceed that stress because a higher fraction of isotropic percentage compared to the crack number occurring in the macroscopic fracture indicates higher failure tendency. Incorporating a stiffness ratio of 1 for the simulation of mathematical sample together with calibrated contact parameter which is the parallel bond of 17MPa enhance modelling of internal stresses thus highlight the effects of stress induced strain.

ACKNOWLEDGMENT

Acknowledgment to the Tertiary Education Trust fund abbreviated as TETFUND." And Federal University of Technology Minna for sponsor and financial support**.**

REFERENCES

[1] Eberhardt, E., Stead, D., Stimpson, B., & Read, R. S. (1998). Identifying crack initiation and propagation thresholds in brittle rock. Canadian geotechnical journal, 35(2), 222-233.

[2] 2 Graham, C. C., Stanchits, S., Main, I. G., & Dresen, G. (2010). Comparison of polarity and moment tensor inversion methods for source analysis of acoustic emission data. International journal of rock mechanics and mining sciences (Oxford, England: 1997), 47(1), 161.

[3] Martin, C. D., & Chandler, N. A. (1994, December). The progressive fracture of Lac du Bonnet granite. In International journal of rock mechanics and mining sciences & geomechanics abstracts (Vol. 31, No. 6, pp. 643-659). Pergamon

[4] Lockner DA, Madden TR. Quasi-static failure growth and shear fracture energy in granite. Nature 1991;350:39–42.

[5] Stanchits, S., Mayr, S., Shapiro, S., & Dresen, G. (2011). Fracturing of porous rock induced by fluid injection. Tectonophysics, 503(1-2), 129-145.

[6] Heinze, T., Galvan, B., & Miller, S. A. (2015). Modeling porous rock fracturing induced by fluid injection. International Journal of Rock Mechanics and Mining Sciences, 77, 133-141..

[7] Fortin, J., Stanchits, S., Dresen, G., & Guéguen, Y. (2006). Acoustic emission and velocities associated with the formation of compaction bands in sandstone. Journal of Geophysical Research: Solid Earth, 111(B10)..

[8] Cho, N., Martin, C. D., & Sego, D. C. (2008). Development of a shear zone in brittle rock subjected to direct shear. International Journal of Rock Mechanics and Mining Sciences, 45(8), 1335-1346.

[9] Dresen, G., Stanchits, S., & Rybacki, E. (2010). Borehole breakout evolution through acoustic emission location analysis. International Journal of Rock Mechanics and Mining Sciences, 47(3), 426-435.

[10] Young, R. P., Nasseri, M. H. B., & Lombos, L. (2012). Imaging the effect of the intermediate principal stress on strength, deformation and transport properties of rocks using seismic methods. True triaxial testing of rocks. Balkema, Taylor and Francisco Group, 167-179.

[11] Potyondy, D. O., & Cundall, P. A. (2004). A bonded-particle model for rock. International journal of rock mechanics and mining sciences, 41(8), 1329-1364.

[12] Itasca, PFCD3D (Particle Flow Code in 3 Dimensions) Manual. Version 4.0 ed. 2004, Minneapolis, Minesota; MN:ICG

[13] Graham, C. C., Stanchits, S., Main, I. G., & Dresen, G. (2010). Comparison of polarity and moment tensor inversion methods for source analysis of acoustic emission data. International journal of rock mechanics and mining sciences (Oxford, England: 1997), 47(1), 161.

[14] Antony, S. J., Olugbenga, A., & Ozerkan, N. G. (2018). Sensing, measuring and modelling the mechanical properties of sandstone. Rock Mechanics and Rock Engineering, 51(2), 451-464.

[15] Nasvi, M. M., Gamage, R. P., & Jay, S. (2012). Geopolymer as well cement and the variation of its mechanical behavior with curing temperature. Greenhouse gases: science and technology, 2(1), 46-58.

[16] Diederichs, M. S., Kaiser, P. K., & Eberhardt, E. (2004). Damage initiation and propagation in hard rock during tunnelling and the influence of near-face stress rotation. International Journal of Rock Mechanics and Mining Sciences, 41(5), 785-812.

[17] Young, R. P., Hazzard, J. F., & Pettitt, W. S. (2000). Seismic and micromechanical studies of rock fracture. Geophysical Research Letters, 27(12), 1767-1770.

[18] Eberhardt, E., Stead, D., & Stimpson, B. (1999). Quantifying progressive pre-peak brittle fracture damage in rock during uniaxial compression. International Journal of Rock Mechanics and Mining Sciences, 36(3), 361-380.Young, "Synthetic structure of industrial plastics (Book style with paper title and editor)," in *Plastics*, 2nd ed. vol. 3, J. Peters, Ed. New York: McGraw-Hill, 1964, pp. 15–64.

[19] W.-K. Chen, *Linear Networks and Systems* (Book style). Belmont, CA: Wadsworth, 1993, pp. 123–135.

[20] H. Poor, *An Introduction to Signal Detection and Estimation*. New York: Springer-Verlag, 1985, ch. 4.